Novel CaO–SiO2 Sorbent and Bifunctional Ni/Co–CaO/SiO2 Complex for Selective H–2 Synthesis from Cellulose

ARTICLE *in* ENVIRONMENTAL SCIENCE & TECHNOLOGY · MARCH 2012

Impact Factor: 5.33 · DOI: 10.1021/es300135d · Source: PubMed

4 AUTHORS, INCLUDING:

Ming Zhao
Tsinghua University
18 PUBLICATIONS **245** CITATIONS
SEE PROFILE

Andrew T Harris
National Health Service
45 PUBLICATIONS **362** CITATIONS
SEE PROFILE

Environmental Science & Technology

Article

pubs.acs.org/est

Novel CaO−SiO_2 Sorbent and Bifunctional Ni/Co−CaO/SiO_2 Complex for Selective H_2 Synthesis from Cellulose

Ming Zhao,*[,†] Xiaoshuang Yang,[†,‡] Tamara L. Church,[†] and Andrew T. Harris*[,†]

[†]Laboratory for Sustainable Technology, School of Chemical and Biomolecular Engineering, The University of Sydney, NSW 2006, Australia

[‡]The Bragg Institute, Australian Nuclear Science and Technology Organisation, Lucas Heights, NSW 2234, Australia

Supporting Information

ABSTRACT: Catalysis- and sorption-enhanced biomass gasification is a promising route to high-purity hydrogen (H_2); however, most CaO-based sorbents for CO_2 capture have poor surface area and mechanical properties, lose carrying capacity over multiple uses, and have insufficient porosity to accommodate extra catalyst sites. We aimed to develop a high-surface-area CaO−SiO_2 framework onto which catalysts could be grafted. The best CaO−SiO_2 sorbent (n_{Ca}/n_{Si} = 2:1) maintained a CaO conversion of 65% even after 50 carbonation−decarbonation cycles, better than commercial micrometer-sized CaO or tailored CaO, because of stabilization via Ca−O−Si interactions and an ordered porous structure. Bimetallic catalyst grains (Ni/Co alloy, <20 nm) could be evenly loaded onto this structure by impregnation. The resulting bifunctional complex produced H_2 at nearly the same rate as a mixture of catalyst and commercial CaO while using less total sorbent/catalyst. Furthermore, this complex was much more durable due to its higher coking resistance and stable structure. After 25 carbonation−decarbonation cycles, the new catalyst−sorbent complex enhanced the H_2 yield from cellulose far more than a mixture of catalyst and commercial CaO did following the same treatment.

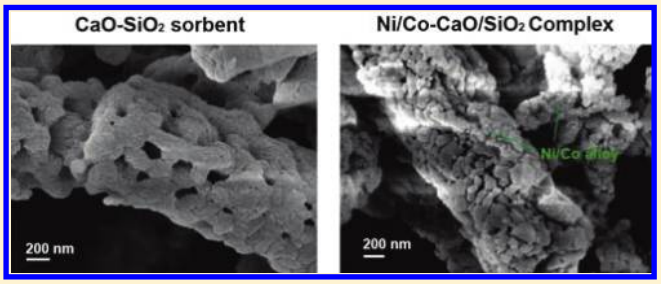

INTRODUCTION

H_2 is an ideal alternative to fossil fuels from the perspective of CO_2 emissions. The gasification of nonedible biomass or organic wastes could provide a sustainable route to large scale H_2 production for a hydrogen economy.[1−3] Biomass is gasified at lower temperature (500−800 °C) than coal because biomass contains more functionalities, and is thus more reactive, than coal.[4−6] At these temperatures, CaO captures CO_2, which drives the water−gas shift reaction to produce more H_2 and thus enhances the H_2 yield from gasification.[7] Reforming catalysts can remove tar during gasification and enrich the gas product in H_2.[8−11] The combination of CaO-based sorbents and reforming catalysts can thus provide CO_2 separation and tar elimination, lower catalyst deactivation, and consequently, produce high purity H_2.[12] Ideally, biomass-derived H_2 should be pure enough to use in devices such as PEM fuel cells.

Natural CaO-based CO_2 sorbents (limestone, dolomite, etc.) have been widely investigated, but their poor mechanical properties cause them to degrade by attrition or elutriation during use in circulating fluidized beds.[13] Furthermore, their sorption capacity decays rapidly over multiple cycles due to sintering.[14,15] Tailored CaO sorbents have been produced, but most maintain only 20−50% of their activity after 50 cycles due to the intrinsic limitations of CaO.[16,17]

An alternative approach is to load CaO onto an inert support.[18] The strengthened structure could hinder sorbent degradation, and the interaction between CaO and the support could mitigate sintering. Moreover, for selective H_2 production, metal catalysts could be doped onto a stable porous CaO−substrate framework. Some sorbent−catalyst composites have been used for hydrocarbon reforming.[19,20] However, CaO does not react readily with common substrate materials, and the high temperatures (>900 °C) required to induce reaction disfavor high surface area materials.[21,22] Additionally, the enhanced stability of supported CaO sorbents comes at the cost of a substrate that does not absorb CO_2.[18] We developed a sol−gel synthesis of porous-SiO_2-supported CaO sorbents (CaO−SiO_2). These were characterized and compared to CaO sorbents in multicycle carbonation−decarbonation tests. We also developed a bifunctional Ni/Co−CaO/SiO_2 complex and investigated its impact on H_2 yield and selectivity in cellulose pyrolysis.

EXPERIMENTAL SECTION

Sorbents. The triblock-copolymer-templated synthesis of mesoporous silica (SBA-15)[23] was modified to introduce CaO. A saturated solution obtained by dissolving $Si(OEt)_4$ (Sigma-Aldrich, 0.025 mol) and $CaCl_2$ (Ajax Finechem, 0.025, 0.05, or 0.075 mol) in 20 mL of absolute ethanol was added dropwise into a mixture of 50 mL of HCl (2 M), 2 g of Pluronic P123

Received: October 27, 2010
Accepted: January 14, 2012
Published: January 17, 2012

   dx.doi.org/10.1021/es300135d | Environ. Sci. Technol. 2012, 46, 2976−2983

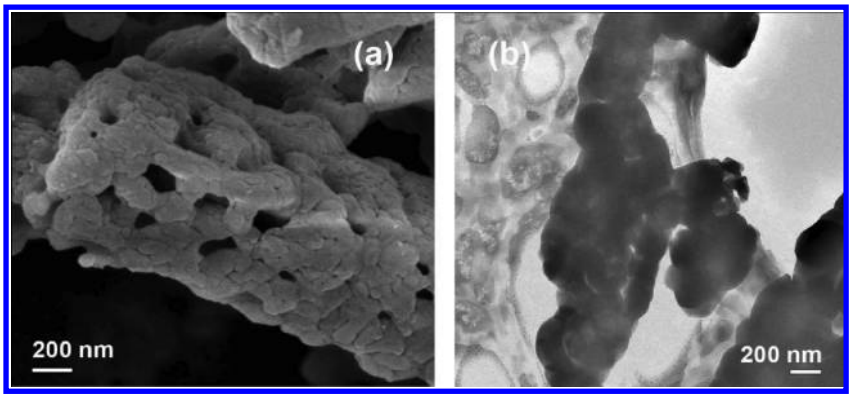

Figure 1. (a) SEM and (b) TEM images of S2.

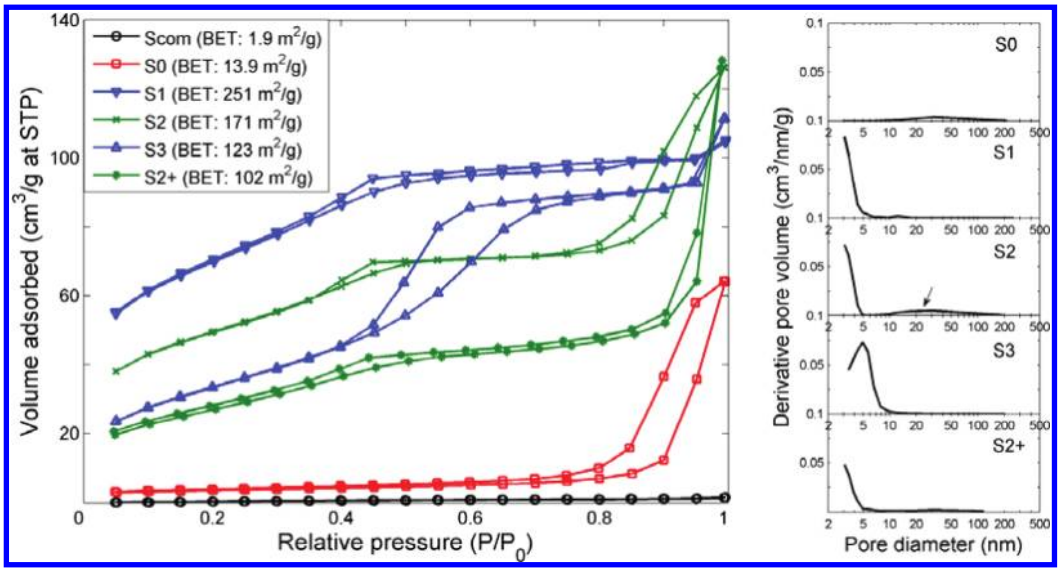

Figure 2. N_2 physisorption analysis of sorbents. Surface area and pore size distribution were calculated from adsorption data.

($PEO_{20}PPO_{70}PEO_{20}$, $M_n \sim 5800$), and $H_2C_2O_4$ (anhydrous, Sigma-Aldrich, $n(H_2C_2O_4) = n(CaCl_2)$). The flask was sealed, and the mixture was stirred for 35 h at 60 °C in an oil bath. The precipitate was washed with distilled water until the pH of the washings approached 7, laid out at room temperature overnight, and dried at 110 °C for 4 h. The obtained powder was calcined at 550 °C ($\partial T/\partial t$ = 2 °C/min) in air for 4 h. The sorbents with n_{Si}/n_{Ca} = 1:1, 1:2, and 1:3 were labeled S1, S2, and S3, respectively. Tailored $CaCO_3$ (S0) was prepared analogously but without $Si(OEt)_4$, and micrometer sized $CaCO_3$ (Scom, Sigma-Aldrich) was used for comparison.

Ni/Co−CaO/SiO$_2$. Our research on mesoporous-silica-supported catalysts revealed that 10 wt% $NiCo_2$ alloy was a superior catalyst for selective H_2 production from cellulose.[24] Here, the same procedure was adopted to form 10 wt% $NiCo_2$ on the surface of $CaO-SiO_2$. The $Ni/Co-CaO/SiO_2$ complex was denoted S2+.

Characterization. N_2 physisorption isotherms were obtained at 77 K (Quantachrome Autosorb iQ). Specific surface areas and pore size distributions were calculated by the Brunauer−Emmett−Teller (BET) and Barrett−Joyner−Halenda (BJH) methods, respectively. Crystallinity was assessed using X-ray diffraction (XRD, SIEMENS D5000, Cu Kα radiation, λ = 0.1542 nm). X-ray photoelectron spectroscopy (XPS, VG ESCALAB 220iXL) recorded the core binding energies of elements in the sorbents. Scanning electron microscopy (FESEM, Zeiss Ultra+) and energy-dispersive X-ray spectroscopy (EDS) were used to qualitatively assess particle morphology and elemental compositions.

Carbonation−Decarbonation. A thermogravimetric analyzer (TA Q5000IR) was used to monitor CO_2 capture and release. Generally, ~3 mg of sorbent was evenly loaded onto a platinum pan to minimize mass transfer effects. Samples were heated in N_2 (60 mL/min) at 20 °C/min to 700 °C and held at this temperature for 5 min to allow complete calcination. Recarbonation occurred when the temperature was lowered to 600 °C, and the gas was switched to 40 mL/min CO_2 in 20 mL/min N_2 for 60 min. The same capture-and-release test was repeated 50×. CaO conversion, χ_{CaO}, was defined as follows:

$$\chi_{CaO} = [n(CO_2)_{absorbed}/n(CaO)] \times 100\% \quad (1)$$

H_2 Production from Cellulose. The as-synthesized S2+ complex was activated in H_2 (25 vol% in Ar) at 700 °C for 60 min to reduce the Ni/Co oxide and decarbonate $CaCO_3-SiO_2$. Methyl cellulose ("cel", Sigma-Aldrich), a component of and model compound for biomass, was decomposed in the presence of activated S2+ in a thermogravimetric analyzer (SDT Q600) that was coupled to a mass spectrometer (ThermoStar GSD301) (TG-MS). H_2 yield and gas product distribution were assessed. S2+ was compared with commercial CaO (Scom) and with 10 wt% $NiCo_2$ supported on SBA-15 ("cat"). These have been described in detail.[12,24]

dx.doi.org/10.1021/es300135d | Environ. Sci. Technol. 2012, 46, 2976−2983

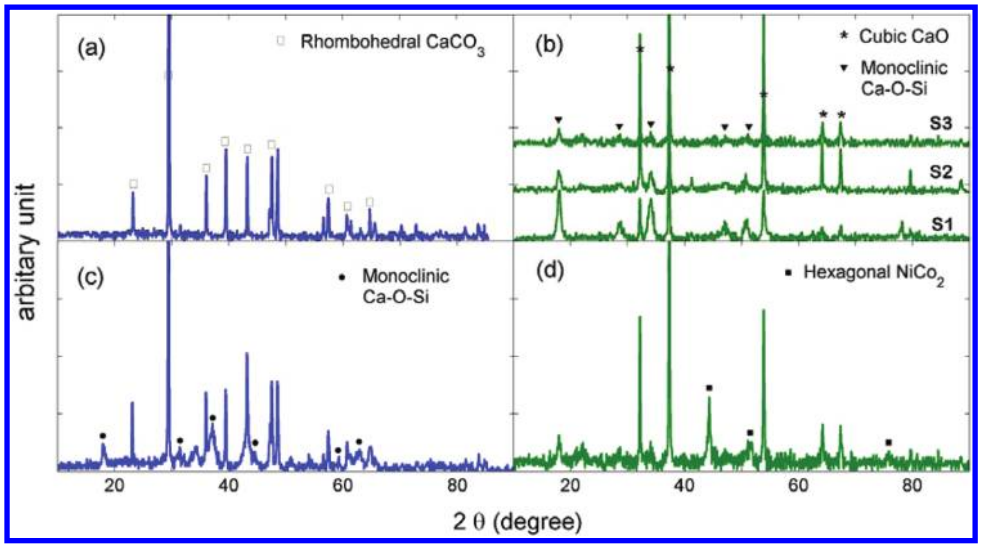

Figure 3. X-ray diffraction patterns of: (a) S2 (representative of S1, S2, S3); (b) S1, S2, and S3 decarbonated in N_2 at 700 °C for 1 h; (c) S2+; and (d) S2+ activated in 25 vol% H_2 at 700 °C for 60 min.

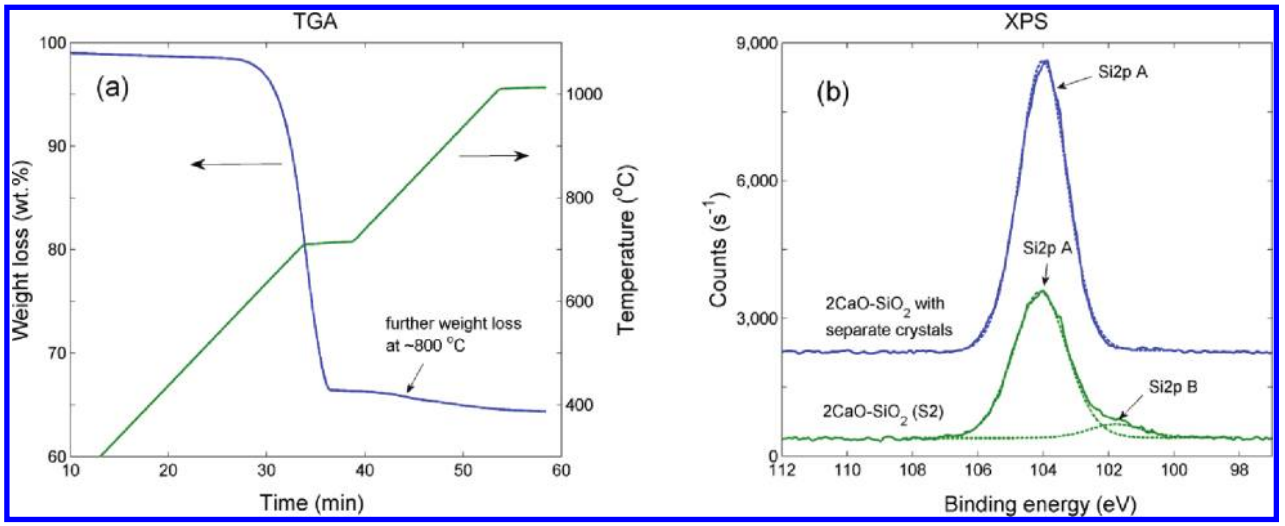

Figure 4. Further evidence of the interaction between CaO and SiO_2 in S2: (a) weight loss of S2 upon calcination in N_2 up to 1000 °C; (b) Si2p region of the XPS spectra of 2CaO−SiO_2 as separate crystals and as S2.

RESULTS AND DISCUSSION

Characterization of CaO−SiO_2 Sorbents. Following an initial failure (see the Supporting Information), we developed a procedure that permitted the integrated condensation of SiO_2 and CaC_2O_4 (eqs 2 and 3). Co-dissolving $Si(OEt)_4$ and $CaCl_2$ in ethanol enabled Ca−O−Si linkages to form through coordination bonds,[25] and the microphase separation of a block-copolymer regulated the porosity of the solid product.[26] A one-fold, integrated framework resulted.

$$Si(OC_2H_5)_4 + 2H_2O \xrightarrow{HCl} SiO_2 + 4C_2H_5OH \quad (2)$$

$$H_2C_2O_4 + CaCl_2 \rightarrow CaC_2O_4 + 2HCl \quad (3)$$

Only S2 (n_{Si}/n_{Ca} = 1:2) had regular shape and an ordered macroporous structure (Figure 1a). In it, Si and Ca were evenly distributed in columnar particles (diameter: 0.5−1 μm, length: 2−4 μm) that were hollow due to connected channels visible in the SEM and TEM images (Figure 1). EDS spectra showed the elements well-distributed on the surface (Supporting Information, Figure S1c).

N_2 physisorption measurements (Figure 2) revealed that most of the pores in the three CaO−SiO_2 sorbents were 2−10 nm in diameter and the average pore size increased with Ca content. Thus, although high CO_2 capture capacity requires high Ca content, excessive Ca decreased porosity; the surface area of S3 was only 123 m^2/g. S1 had the highest surface area (251 m^2/g), but this was mainly from the Si-dominated SBA-15-like mesostructure. Besides the relatively uniform mesopores, S2 also had macropores, in contrast to S1 and S3. These macropores might contribute to the hollow structure of S2 (Figure 1a). S2+ showed a similar pore size distribution to S2, but the addition of metals decreased porosity and surface area (102 m^2/g for S2+; cf. 171 m^2/g for S2). Without Si content, S0 had low porosity and surface area (13.9 m^2/g) and a broad pore size distribution.

Figure 3 depicts the X-ray diffraction patterns of CaO−SiO_2 samples. Only one phase (rhombohedral $CaCO_3$[16]) was observed for S1−3 (Figure 3a), indicating that reaction 4 occurred. After decarbonation (eq 5), the sorbents contained cubic CaO plus varying amounts of a second, monoclinic phase

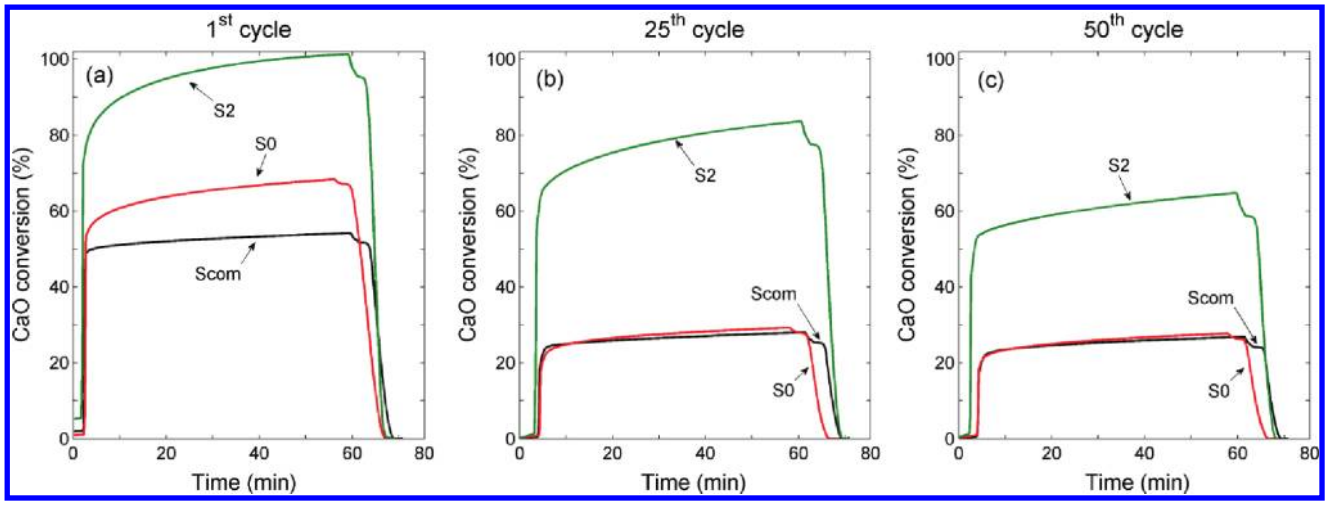

Figure 5. Carbonation−decarbonation rates in (a) 1st, (b) 25th, and (c) 50th cycles. Carbonation for 60 min at 600 °C under 66.7 vol% CO_2 in N_2; calcination for 5 min at 700 °C under N_2.

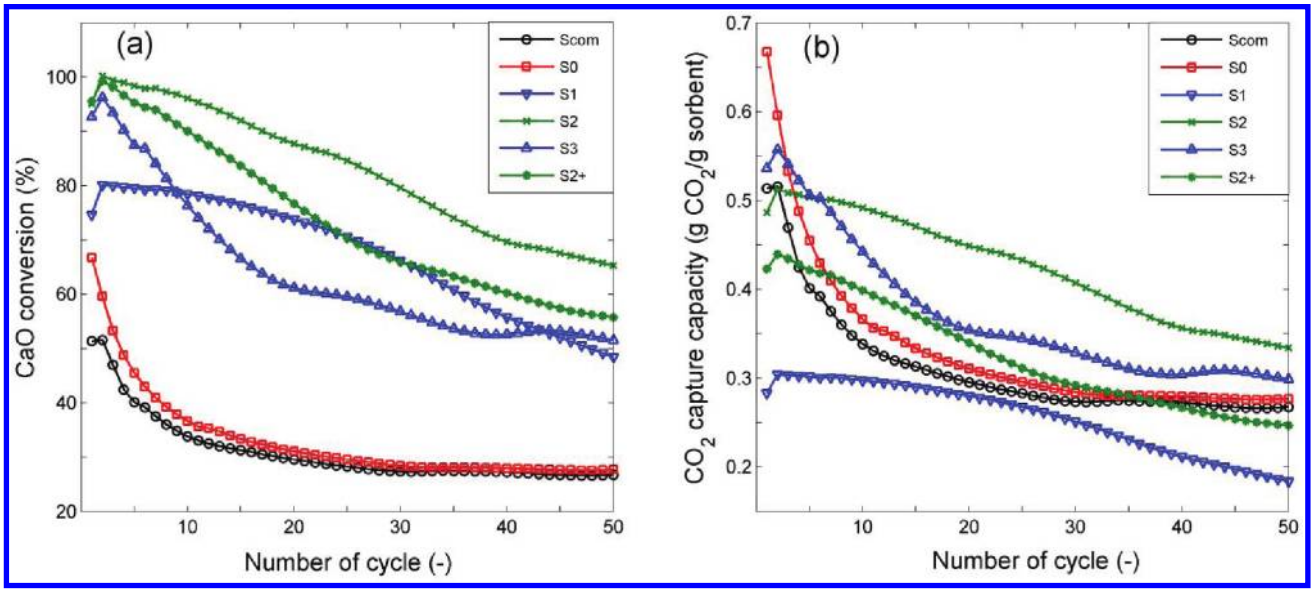

Figure 6. (a) χ_{CaO} and (b) CO_2 capture capacity through 50 cycles. Carbonation for 60 min at 600 °C under 66.7 vol% CO_2 in N_2; calcination for 5 min at 700 °C under N_2.

(Figure 3b) that was not $CaCO_3$, CaO, SiO_2 (quartz), $CaSiO_3$ (wollastonite), or Ca_2SiO_4. Although the new monoclinic phase could not be identified, it likely contained oxide and/or carbonate anions, as well as Ca−O−Si bonds. This crystalline phase was absent until decarbonation, so it may have required CaO to form or have been amorphous before decarbonation. Regardless, because the compound was neither pure CaO nor SiO_2, its presence demonstrated the formation of a stable interaction between these compounds, presumably with Ca−O−Si bonds.

$$CaC_2O_4 \xrightarrow{<600^\circ C} CaCO_3 + CO \quad (4)$$

$$CaCO_3 \xrightarrow{700^\circ C, N_2} CaO + CO_2 \quad (5)$$

Further evidence to support this assignment is shown in Figure 4. S2 lost 1.6% of its weight when heated to 800 °C (Figure 4a), suggesting that it contained some carbonate ions that were stable at 700 °C. At least one calcium silicate carbonate, spurrite, is more stable to decarbonation than $CaCO_3$.[27] Figure 4b compares the XPS spectra of $2CaO{-}SiO_2$ synthesized by two different procedures (see the Supporting Information). S2 showed a secondary Si2p core binding energy at 101.55 eV, indicating a change of valence electron charge of Si due to bonding that resembled Si−O−Ca.[28] Kaneko[29] reported a Si2p binding energy for $2CaO{\cdot}SiO_2$ (silicate form) at 101.9 eV, suggesting that this Si−O−Ca network is different from silicate.

Thus, the new sol−gel method yielded a porous structure underpinned by a Ca−O−Si network that formed in solution at low temperature, rather than at the high temperatures required for the direct reaction between CaO and SiO_2.[30] Despite having interactions between CaO and SiO_2, these sorbents retained numerous active CaO sites (vide infra).

Durability. To be useful for CO_2 capture in biomass gasification, a sorbent must absorb and release CO_2 repeatedly, with minimal decay in activity. Figure 5 shows the CO_2 absorption profiles of Scom, S0, and S2 in the first, 25th, and 50th cycles. These are compared based on χ_{CaO} because of their

dx.doi.org/10.1021/es300135d | Environ. Sci. Technol. 2012, 46, 2976−2983

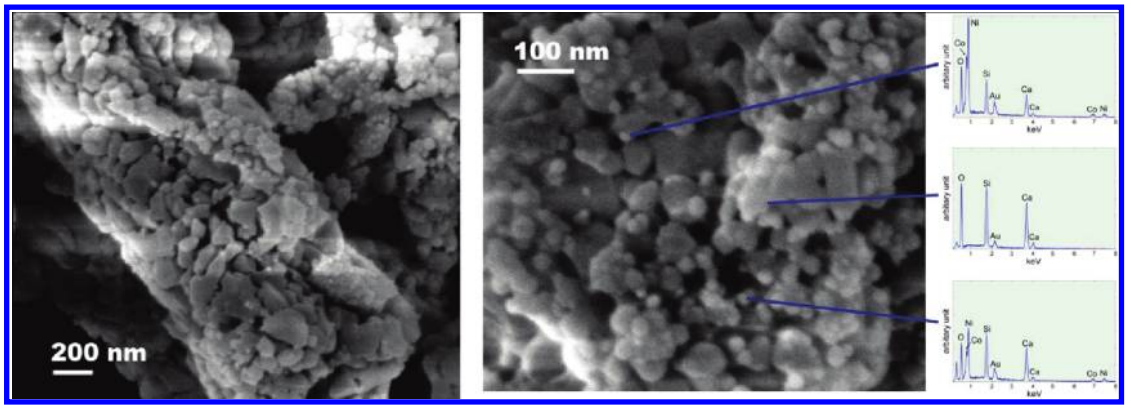

Figure 7. SEM images of S2+ (a) before and (b) after activation (25 vol% H_2 in N_2, 700 °C, 60 min). The accompanying spectra show EDS spectra.

different chemical compositions (see the Experimental Section). All sorbents exhibited reduced χ_{CaO} after multiple cycles. Surface area loss through sintering is the primary factor influencing conversion,[15,31] as was visible in the SEM images of the fresh and 25-times-cycled sorbents (Supporting Information, Figure S3). The different sintering behavior of the sorbents correlated to both the absorption kinetics in individual cycles (Figure 5) and the decay trends (Figure 6).

In an individual cycle, each sorbent underwent two-phase carbonation: a fast, kinetically controlled phase was followed by a slow, diffusion-controlled phase.[16,32] Fresh Scom (Figure 5a) transitioned abruptly between the phases, suggesting that it was least affected by surface diffusion, possibly due to its nonporosity; in comparison, the tailored (S0) and SiO_2-supported CaO (S2) showed gradual transitions from the chemical-reaction-controlled phase to the diffusion-controlled phase as CO_2 diffused through their pores. S2, which benefited from a larger surface area and well-distributed active sites, approached complete carbonation, with ∼95% CaO converted. The bulky, nonporous crystals of Scom rendered nearly half of its CaO sites inaccessible ($\chi_{CaO(max)}$ = 52%). S0 reached 67% conversion, making it clearly better than Scom but much worse than S2. The reactivity of S0 was likely impeded by its low surface area and poor porosity (Figure 2). The 5% of Ca sites that were inaccessible in S2 were likely fixed in the SiO_2 substrate, possibly as part of an oxide/carbonate (vide supra). After 25 cycles (Figure 5b), a significant drop in conversion was observed for Scom and S0, in both of which only ∼30% of the CaO remained accessible for carbonation, whereas S2 still reached 85% conversion. The poor activities of Scom and S0 in the 25th cycle reflected the morphology changes in these sorbents (Supporting Information, Figures S3). Sintering occurred as atoms moved across particle boundaries, giving rise to grain growth.[33] The enlarged Scom particles exhibited some amorphous character and S0, also subject to the sintering propensity of pure CaO, lost most of its porosity and surface area. Conversely, the porosity of S2 was well-maintained, although sintering between particles was also observed following the multiple high-temperature trials. A further drop in CaO conversion was observed in the 50th cycle for all sorbents, though S2 maintained 65% activity.

Figure 6a compares the decay in the sorbent reactivity through 50 reaction cycles. The unsupported sorbents (Scom and S0) showed typical, significant decays in conversion over the first 25 cycles before approaching asymptotic decay. S0 showed the advantages of tailored CaO during the first 10 cycles but degraded thereafter. Two supported sorbents, S1 and S2, exhibited steady linear decreases in CaO conversion; whereas S3 had a similar decay profile to Scom and S0, albeit with much higher conversions. Several factors contributed to the different decay behaviors of these sorbents. Decarbonated S1 and S2 both contained significant amounts of a Ca−O−Si bonded species (see Figure 3b), which would have hindered the motion of atoms on the support, significantly slowing sintering. Accordingly, the used S2 showed the least serious sintering. On the other hand, Ca−O groups immobilized in this way may have poor or no reactivity toward CO_2; therefore, S1, which showed the most such interactions, reached substantially lower χ_{CaO} (80%) than did S2, even on the second cycle where S1 exhibited maximum conversion due to self-reactivation in the first cycle.[34] The reactivity of S3, which showed minimal evidence for Ca−O−Si interactions, decayed in χ_{CaO} more rapidly than those of S1 and S2 despite that its second-cycle conversion (94%) was close to that of S2 (>99%). Therefore, there was a trade-off between CaO available for absorption and stabilizing interactions with the support, with the balance being optimal when n_{Si}/n_{Ca} = 1:2. The evenly channelled structure of S2 may also have contributed to its thermal stability. The CaO conversion of S2 in the 50th cycle reached ∼65%.

Although the supported sorbents showed greatly enhanced sintering resistance, the presence of Si, which does not absorb CO_2, reduces the CO_2 capture capacity per unit sorbent mass. Figure 6b compares the sorbents on this basis. In the first few cycles, only tuned CaO (S0) and high-Ca S3 took up more CO_2 than S2. However, the CO_2 uptake per unit mass of S2 surpassed those of S0 and S3 at the fourth and sixth cycle, respectively, due to their dramatic decay in CO_2 uptake upon repeated reuse. Thus, S2 captured more CO_2 for most of its cyclic use, retaining a high capacity of 0.33 g CO_2/g sorbent at the end of trials. In total, S2 absorbed 21.2 g CO_2/g sorbent, whereas Scom absorbed 15.5 g CO_2/g sorbent.

Metal Loading and H_2 Production from Biomass. Impregnation by an ethanol solution of Ni and Co nitrates and subsequent drying and calcination did not noticeably influence the structure of S2; S2+ had similar morphology to S2 (Figure 7). The XRD pattern of S2+ (Figure 3c) indicated that cubic $NiCo_2O_4$ was formed on the $CaCO_3$−SiO_2 support. Activating S2+ under H_2 at 700 °C produced evenly distributed, fairly uniform particles (<20 nm), which XRD and EDS analyses identified as a Ni/Co alloy (Figures 3d and 7).[24] S2+ had a lower BET surface area than S2 (102 m^2/g) due to the addition of metals to S2, which also caused the collapse of some meso- and macropores (Figure 2). Accordingly, the sorption ability of

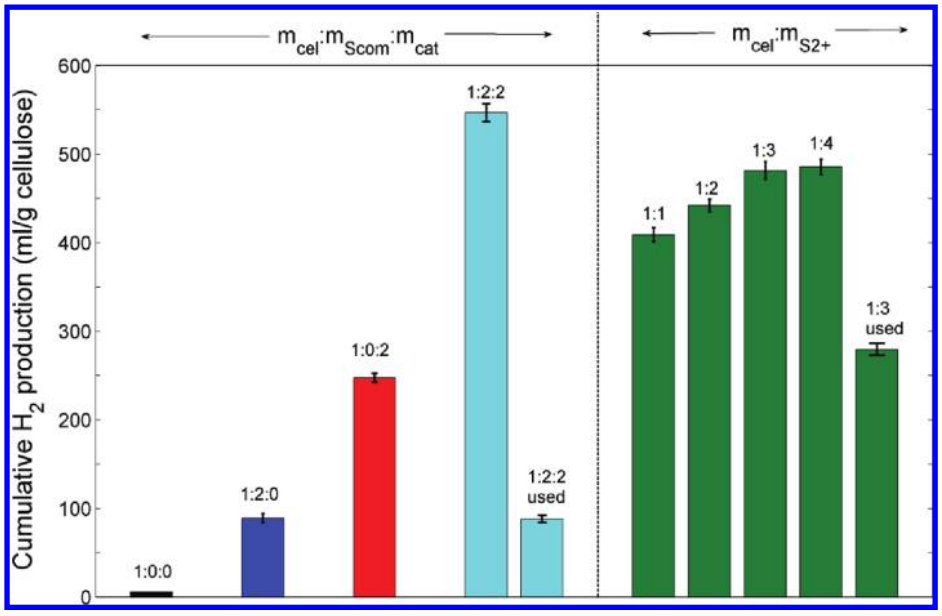

Figure 8. H_2 yield (250−550 °C) from cellulose pyrolysis (40 °C/min to 800 °C, in 500 mL/min Ar) using various additives.

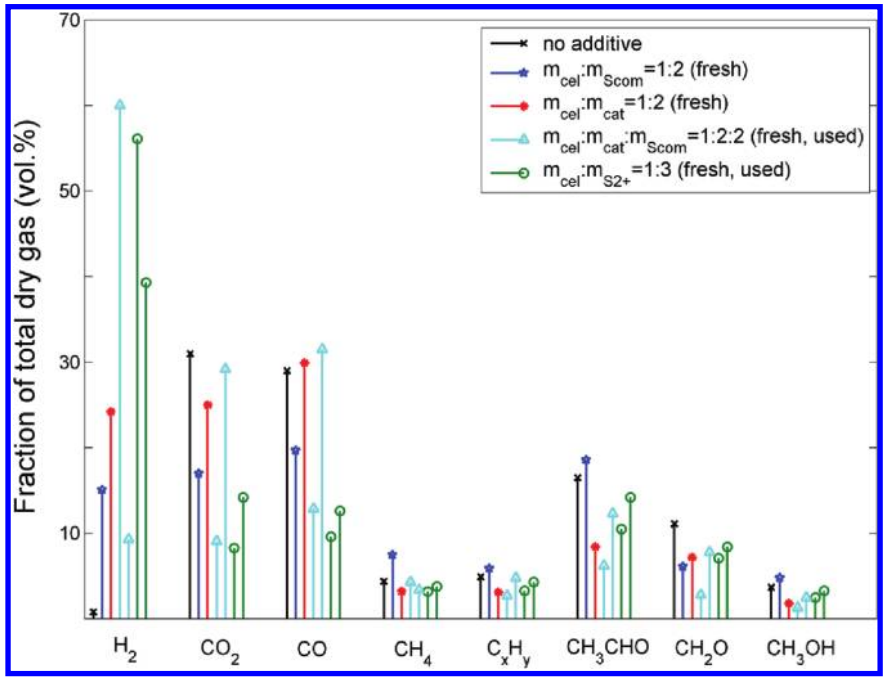

Figure 9. H_2 selectivity (250−550 °C) from cellulose pyrolysis.

CaO on S2+ decreased to χ_{CaO} = 96 and 56% after one and 50 cycles, respectively (Figure 6).

TG-MS can semiquantitatively assess the generation rate, yield, and distribution of the gas products evolved from cellulose decomposition, giving data that is not absolute but that can be accurately compared.[8,9,12,24] Figure 8 shows the cumulative H_2 yields measured in the presence of various catalysts over the range 250−550 °C. Volumetric quantities (mL/g or mL/min/g) were calculated for gases at room temperature (~25 °C) and atmospheric pressure (1 atm). Combining a sorbent and catalyst ($m_{cel}/m_{cat}/m_{Scom}$ = 1:2:2) increased the H_2 yield from pyrolysis to 527 mL/g cellulose compared with sorbent- or catalyst-only processes (100 and 255 mL/g cellulose, respectively). The optimal loading of S2+ was m_{S2+}/m_{cel} = 3:1, when the output of H_2 reached 486 mL/g. This significantly surpassed the performance of either catalyst or sorbent independently, and approached that of their mixture, despite that less additive was used ($m_{additive}/m_{cel}$ = 3:1, cf. 4:1 for the mixture).

The advantages of S2+ were most striking when partially spent catalyst/sorbents were tested. S2+ was subjected to 25 carbonation (30 min at 600 °C under 66.7 vol% CO_2 in N_2) and decarbonation (5 min at 700 °C under N_2) cycles and then applied in cellulose pyrolysis (Figure 8). The H_2 yield was 280 mL/g cellulose, which was 42% lower than from fresh S2+ but still higher than pyrolysis in the presence of catalyst or fresh sorbent alone. When cat+Scom was subjected to an identical treatment, its ability to enhance H_2 production was drastically reduced; it gave only 88 mL/g cellulose when applied to cellulose pyrolysis. Thus, the spent mixture produced 83% less

dx.doi.org/10.1021/es300135d | Environ. Sci. Technol. 2012, 46, 2976−2983

H_2 than the fresh mixture had; this was less than the pyrolysis of cellulose without a sorbent. The sintered sorbent may have enveloped some Ni/Co particles, making them inaccessible as tar-cracking catalysts.

Both S2+ and the mixture (cat+Scom) significantly amplified H_2 selectivity from cellulose pyrolysis (Figure 9). S2+ gave 56 vol% H_2 from cellulose pyrolysis (cf. 61 vol% for the mixture). Most unwanted species could be minimized using the mixture, though the amounts of some oxygen-containing compounds increased slightly. CaO, a basic catalyst, promoted tar-degradation, while the Ni/Co alloy catalyzed the cracking of smaller tar-degradation products. S2+ combined these active sites into one porous particle, reducing the importance of molecular transport in the system. Meanwhile, compared with the mixture, S2+ showed a slight decrease in CO_2 and CO generation rate under 550 °C, suggesting that the integrated sorbent/catalyst promoted the water−gas shift reaction more effectively than mixture. This was likely the reason why S2+ gave only a bit less H_2 production than mixture even though SBA-15 supported catalysts had much higher surface area.

The superior resilience of CaO−SiO_2 returned advantages as the experiment continued; partially spent S2+ gave 39% H_2, whereas the partially spent cat+Scom mixture gave only 9%. The rapid degradation of commercial CaO in CO_2 capture capacity over multiple cycles was clearly important here. Furthermore, S2+ exhibited the lowest char yield (6.7 wt%) at 800 °C, suggesting a superior coking resistance. This was maintained after many carbonation−decarbonation cycles; cellulose pyrolysis in the presence of partially spent S2+ produced 6.8 wt% char at 800 °C. CaO is active for char gasification by H_2O and CO_2,[12] and the integration of CaO and Ni/Co alloy sites allows CaO to remove carbon from the catalyst particles. This enhanced gasification and minimized catalyst.

■ ASSOCIATED CONTENT

Supporting Information

Additional synthesis details for and SEM/EDS images of sorbents are presented, as are more information and results of cellulose pyrolysis in TG-MS in presence of various additives. This material is available free of charge via the Internet at http://pubs.acs.org.

■ AUTHOR INFORMATION

Corresponding Author

*Phone: 61-2-9351-3397 (M.Z.); 61-2-9351-2926 (A.T.H.). Fax: 61-2-9351-2854 (A.T.H.). E-mail: ming.zhao@sydney.edu.au (M.Z.); andrew.harris@sydney.edu.au (A.T.H.).

Notes

The authors declare no competing financial interest.

■ ACKNOWLEDGMENTS

M.Z. thanks the Chinese Scholarship Council and the University of Sydney for postgraduate scholarships. We are grateful to the Australian Research Council (DP0666488) and E.ON AG for support.

■ REFERENCES

(1) Balat, M.; Balat, M. Political, economic and environmental impacts of biomass-based hydrogen. *Int. J. Hydrogen Energy* **2009**, *34* (9), 3589−3603.

(2) Huber, G. W.; Iborra, S.; Corma, A. Synthesis of transportation fuels from biomass: chemistry, catalysts, and engineering. *Chem. Rev.* **2006**, *106* (9), 4044−4098.

(3) Tanksale, A.; Beltramini, J. N.; Lu, G. M. A review of catalytic hydrogen production processes from biomass. *Renewable Sustainable Energy Rev.* **2010**, *14* (1), 166−182.

(4) Hauserman, W. B. High-yield hydrogen production by catalytic gasification of coal or biomass. *Int. J. Hydrogen Energy* **1994**, *19* (5), 413−419.

(5) Kinoshita, C. M.; Wang, Y.; Zhou, J. Tar formation under different biomass gasification conditions. *J. Anal. Appl. Pyrolysis* **1994**, *29* (2), 169−181.

(6) Aznar, M. P.; Caballero, M. A.; Gil, J.; Martin, J. A.; Corella, J. Commercial steam reforming catalysts to improve biomass gasification with steam-oxygen mixtures: 2. catalytic tar removal. *Ind. Eng. Chem. Res.* **1998**, *37* (7), 2668−2680.

(7) Harrison, D. P. Sorption-enhanced hydrogen production: a review. *Ind. Eng. Chem. Res.* **2008**, *47* (17), 6486−6501.

(8) Zhao, M.; Florin, N. H.; Harris, A. T. Mesoporous supported cobalt catalysts for enhanced hydrogen production during cellulose decomposition. *Appl. Catal., B* **2010**, *97* (1−2), 142−150.

(9) Zhao, M.; Florin, N. H.; Harris, A. T. The influence of supported Ni catalysts on the product gas distribution and H_2 yield during cellulose pyrolysis. *Appl. Catal., B* **2009**, *92* (1−2), 185−193.

(10) Sutton, D.; Kelleher, B.; Ross, J. R. H. Review of literature on catalysts for biomass gasification. *Fuel Process. Technol.* **2001**, *73* (3), 155−173.

(11) Han, J.; Kim, H. The reduction and control technology of tar during biomass gasification/pyrolysis: an overview. *Renewable Sustainable Energy Rev.* **2008**, *12* (2), 397−416.

(12) Zhao, M.; Yang, X.; Church, T. L.; Harris, A. T. Interaction between a bimetallic Ni−Co catalyst and micrometer-sized CaO for enhanced H_2 production during cellulose decomposition. *Int. J. Hydrogen Energy* **2011**, *36* (1), 421−431.

(13) Manovic, V.; Anthony, E. J. Long-term behavior of CaO-based pellets supported by calcium aluminate cements in a long series of CO_2 capture cycles. *Ind. Eng. Chem. Res.* **2009**, *48* (19), 8906−8912.

(14) Wang, J.; Manovic, V.; Wu, Y.; Anthony, E. J. A study on the activity of CaO-based sorbents for capturing CO_2 in clean energy processes. *Appl. Energy* **2010**, *87* (4), 1453−1458.

(15) Sun, P.; Grace, J. R.; Lim, C. J.; Anthony, E. J. The effect of CaO sintering on cyclic CO_2 capture in energy systems. *AIChE J.* **2007**, *53* (9), 2432−2442.

(16) Yang, Z.; Zhao, M.; Florin, N. H.; Harris, A. T. Synthesis and characterization of CaO nanopods for high temperature CO_2 Capture. *Ind. Eng. Chem. Res.* **2009**, *48* (24), 10765−10770.

(17) Liu, W.; Low, N. W. L.; Feng, B.; Wang, G.; Diniz da Costa, J. C. Calcium Precursors for the production of CaO sorbents for multicycle CO_2 Capture. *Environ. Sci. Technol.* **2010**, *44* (2), 841−847.

(18) Huang, C.-H.; Chang, K.-P.; Yu, C.-T.; Chiang, P.-C.; Wang, C.-F. Development of high-temperature CO_2 sorbents made of CaO-based mesoporous silica. *Chem. Eng. J.* **2010**, *161* (1−2), 129−135.

(19) Satrio, J. A.; Shanks, B. H.; Wheelock, T. D. Development of a novel combined catalyst and sorbent for hydrocarbon reforming. *Ind. Eng. Chem. Res.* **2005**, *44* (11), 3901−3911.

(20) Albrecht, K. O.; Satrio, J. A.; Shanks, B. H.; Wheelock, T. D. Application of a combined catalyst and sorbent for steam reforming of methane. *Ind. Eng. Chem. Res.* **2010**, *49* (9), 4091−4098.

(21) Li, Z.-s.; Cai, N.-s.; Huang, Y.-y. Effect of preparation temperature on cyclic CO_2 capture and multiple carbonation−calcination cycles for a new Ca-based CO_2 Sorbent. *Ind. Eng. Chem. Res.* **2006**, *45* (6), 1911−1917.

(22) Martavaltzi, C. S.; Lemonidou, A. A. Development of new CaO based sorbent materials for CO_2 removal at high temperature. *Microporous Mesoporous Mater.* **2008**, *110* (1), 119−127.

(23) Zhao, D.; Feng, J.; Huo, Q.; Melosh, N.; Fredrickson, G. H.; Chmelka, B. F.; Stucky, G. D. Triblock copolymer syntheses of mesoporous silica with periodic 50 to 300 angstrom pores. *Science* **1998**, *279* (5350), 548−552.

(24) Zhao, M.; Church, T. L.; Harris, A. T. SBA-15 supported Ni-Co bimetallic catalysts for enhanced hydrogen production during cellulose decomposition. *Appl. Catal., B* **2011**, *101* (3−4), 522−530.
(25) Rösch, L.; John, P.; Reitmeier, R. *Silicon Compounds, Organic*. In *Ullmann's Encyclopedia of Industrial Chemistry*; Wiley-VCH Verlag GmbH & Co. KGaA: Weinheim, Germany, 2000.
(26) Yang, P.; Zhao, D.; Margolese, D. I.; Chmelka, B. F.; Stucky, G. D. Generalized syntheses of large-pore mesoporous metal oxides with semicrystalline frameworks. *Nature* **1998**, *396* (6707), 152−155.
(27) Glasser, F. P. The formation and thermal stability of spurrite, $Ca_5(SiO_4)_2CO_3$. *Cem. Concr. Res.* **1973**, *3* (1), 23−28.
(28) Veal, B. W.; Lam, D. J.; Paulikas, A. P.; Ching, W. Y. XPS study of CaO in sodium silicate glass. *J. Non-Cryst. Solids* **1982**, *49* (1−3), 309−320.
(29) Kaneko, Y.; Suginohara, Y. Observation of Si2p binding energy by ESCA and determination of O, O^- and O^{2-}ions in silicates. *Nippon Kinzoku Gakkaishi* **1978**, *42* (3), 285−289.
(30) Izquierdo-Barba, I.; Salinas, A. J.; Vallet-Regí, M. In vitro calcium phosphate layer formation on sol-gel glasses of the $CaO-SiO_2$ system. *J. Biomed. Mater. Res.* **1999**, *47* (2), 243−250.
(31) Fennell, P. S.; Pacciani, R.; Dennis, J. S.; Davidson, J. F.; Hayhurst, A. N. The effects of repeated cycles of calcination and carbonation on a variety of different limestones, as measured in a hot fluidized bed of sand. *Energy Fuels* **2007**, *21* (4), 2072−2081.
(32) Florin, N. H.; Harris, A. T. Screening CaO-based sorbents for CO_2 capture in biomass gasifiers. *Energy Fuels* **2008**, *22* (4), 2734−2742.
(33) Kingery, W. D.; Bowen, H. K.; Uhlmann, D. R. *Introduction to Ceramics*, 2nd ed.; John Wiley & Sons, Academic Press: New York, 1976.
(34) Manovic, V.; Anthony, E. J. Thermal activation of CaO-based sorbent and self-reactivation during CO_2 capture looping cycles. *Environ. Sci. Technol.* **2008**, *42* (11), 4170−4174.